Non-Hermitian Phase Transition from a Polariton Bose-Einstein Condensate to a Photon Laser

Ryo Hanai,[1,2,*] Alexander Edelman,[1,3] Yoji Ohashi,[4] and Peter B. Littlewood[1,3]
[1]James Franck Institute and Department of Physics, University of Chicago, Chicago, Illinois, 60637, USA
[2]Department of Physics, Osaka University, Toyonaka 560-0043, Japan
[3]Materials Science Division, Argonne National Laboratory, Argonne, Illinois 60439, USA
[4]Department of Physics, Keio University, Yokohama 223-8522, Japan

(Received 4 September 2018; published 8 May 2019)

We propose a novel mechanism for a nonequilibrium phase transition in a $U(1)$-broken phase of an electron-hole-photon system, from a Bose-Einstein condensate of polaritons to a photon laser, induced by the non-Hermitian nature of the condensate. We show that a (uniform) steady state of the condensate can always be classified into two types, namely, arising either from lower or upper-branch polaritons. We prove (for a general model) and demonstrate (for a particular model of polaritons) that an exceptional point where the two types coalesce marks the end point of a first-order-like phase boundary between the two types, similar to a critical point in a liquid-gas phase transition. Since the phase transition found in this paper is not in general triggered by population inversion, our result implies that the second threshold observed in experiments is not necessarily a strong-to-weak-coupling transition, contrary to the widely believed understanding. Although our calculation mainly aims to clarify polariton physics, our discussion is applicable to general driven-dissipative condensates composed of two complex fields.

DOI: 10.1103/PhysRevLett.122.185301

The phenomenon of macroscopic condensation has been one of the principal topics in modern condensed matter physics and optics [1]. The central example is, of course, Bose-Einstein condensation (BEC), which has been observed in various systems, ranging from atomic gases [2,3], liquid ^{4}He [4], exciton polaritons [5–8], magnons [9–11], photons [12], to plasmonic-lattice polaritons [13]. In these systems, thermalization plays a crucial role in achieving macroscopic occupation of the lowest energy level. A photon laser [14,15], in contrast, is a nonequilibrium condensate, where the population inversion in an optical gain medium induces macroscopic coherence.

The semiconductor microcavity system [5–8] provides a unique opportunity to study similarities and differences of these two classes of condensation phenomena [16], since it can exhibit both [17], by tuning the pump power. At low pump power, where the strong light-matter coupling enables hybrid light-matter quasiparticles called polaritons to form, their thermalization is efficient due to relaxation processes such as stimulated scattering. This makes it possible, once the pump power exceeds a certain threshold, for the system to exhibit macroscopic coherence among polaritons to turn into a polariton BEC [5]. At even higher power, in contrast, the system operates in the weak light-matter coupling regime as a vertical-cavity surface-emitting laser (VCSEL), a type of a photon laser, with electrons and holes acting as a gain medium. Interestingly, a number of experiments [18–29] have observed a second threshold between the former and latter regimes, which has been traditionally interpreted as a strong-to-weak coupling phase transition.

This two-threshold behavior presents a theoretical challenge, however. The normal-to-lasing transition is associated with breaking a $U(1)$ symmetry, but the polariton BEC is already in a $U(1)$-broken phase. Thus, there seems to be no good reason to expect a second phase transition. Indeed, to our knowledge, all theories to date predict a crossover [30–34].

In this Letter, we propose a novel mechanism for a phase transition in the $U(1)$-broken phase, triggered by the non-Hermitian nature of the out-of-equilibrium condensate. Starting from the equation of motion of a microscopic model, we show that the steady states of a two-component condensate of electron-hole pairs and photons can formally be classified into two types of solutions, corresponding to condensation into different branches of the polariton spectrum. We find that an exceptional point (EP), where the two solutions coalesce [35–43], may appear due to the non-Hermiticity of the equation of motion. We prove and demonstrate that this is the end point of a first-order-like phase transition line between the two solutions, analogous to a critical point in a liquid-gas phase diagram. Based on these results, we propose a phase diagram of an electron-hole-photon system depicted in Fig. 1. Our theory points out the possibility of both the crossover and phase transition from polariton BEC to VCSEL depending on the experimental settings such as detuning and the pump power, and provides a possible new interpretation to the

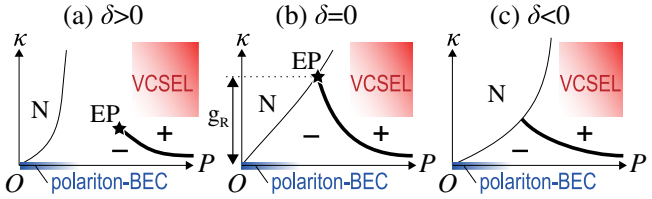

FIG. 1. Proposed phase diagram of a driven-dissipative electron-hole-photon gas, in terms of the photon decay rate κ and the pump power P. (a) Blue detuning. (b) On resonance. (c) Red detuning. "$-(+)$" represents the "$-(+)$"-solution phase, "N" represents the normal phase, "EP" is the exceptional point, and g_R is the Rabi splitting. The thick (thin) solid line represents the phase boundary in the condensed phase (between the normal and the condensed phase).

second threshold as a signal of a lower to upper branch transition. These physics, although derived mainly with microcavity polaritons in mind, should be applicable to other driven-dissipative many-body systems with coupled order parameters, e.g., atoms in a double-well potential [44–46], a supersolid realized in two-crossed cavity [47], or a plasmonic-lattice-polariton BEC [13].

We use a microscopic model schematically shown in Fig. 2 [32–34,48], which has been shown to capture both the essential physics of the BEC state and the VCSEL [49], as well as to give a semiquantitative agreement [48] with photoluminescence experiments [21,50–52]. The system is composed of electrons, holes, and cavity photons, which are coupled to an electron-hole bath and a photon vacuum. Electrons (holes) are incoherently pumped to the system from the bath at a rate $\gamma_{e(h)}$. The injected electrons and holes Coulomb interact with each other and create (annihilate) photons by pair annihilation (creation). The photons leak out to the vacuum with the decay rate κ, driving the system into a nonequilibrium steady state. The explicit expression for the Hamiltonian H is given in the Supplemental Material (SM) [53].

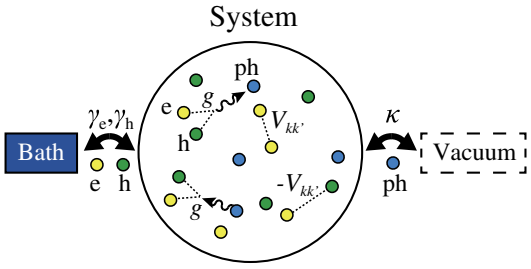

FIG. 2. Model driven-dissipative electron-hole-photon gas. The system is attached to an electron-hole bath and a photon vacuum. Electrons (holes) are incoherently supplied to the system with the rate $\gamma_{e(h)}$. In the system, the injected electrons ("e") and holes ("h") repulsively (e-e, h-h) and attractively (e-h) interact with the Coulomb potential $V_{k-k'} = e^2/(2\epsilon|\boldsymbol{k}-\boldsymbol{k}'|)$. The electrons and holes pair-annihilate (create) to create (annihilate) cavity photons ("ph") via the dipole coupling g. The created photons in the cavity leak out to the vacuum with the decay rate κ.

We apply the Keldysh Green's function method [54] to the model. As shown in the SM [53], the dynamics of the electron-hole dipole polarization $p_{\boldsymbol{k}}(\boldsymbol{r},t)$ and the electron (hole) density $n_{\boldsymbol{k},\sigma=e(h)}(\boldsymbol{r},t)$ obeys the generalized Boltzmann equation [55],

$$i\hbar\partial_t p_{\boldsymbol{k}}(\boldsymbol{r},t) = \left(\varepsilon_{\boldsymbol{k},e} + \varepsilon_{\boldsymbol{k},h} - \frac{\hbar^2\nabla^2}{4m_{eh}} - 2i\gamma\right) p_{\boldsymbol{k}}(\boldsymbol{r},t) - \sum_{\boldsymbol{k}'} L_{\boldsymbol{k},\boldsymbol{k}'}(\boldsymbol{r},t)\Delta_{\boldsymbol{k}'}(\boldsymbol{r},t), \tag{1}$$

$$\partial_t n_{\boldsymbol{k},\sigma}(\boldsymbol{r},t) + \boldsymbol{v}_{\boldsymbol{k},\sigma}\cdot\nabla n_{\boldsymbol{k},\sigma}(\boldsymbol{r},t) = -\frac{2\gamma_\sigma}{\hbar} n_{\boldsymbol{k},\sigma}(\boldsymbol{r},t) + I_{\boldsymbol{k},\sigma}(\boldsymbol{r},t). \tag{2}$$

Here, $\varepsilon_{\boldsymbol{k},e(h)} = \hbar^2\boldsymbol{k}^2/(2m_{e(h)}) + E_g/2$ is the dispersion of the electron (hole) in the conduction (valence) band, where $m_{e(h)}$ is the effective mass of electrons (holes). E_g is the energy gap of the semiconductor material. $m_{eh} = 2m_e m_h/(m_e+m_h)$ is twice the reduced mass of an electron and a hole, and $\boldsymbol{v}_{\boldsymbol{k},e(h)} = \hbar\boldsymbol{k}/m_{e(h)}$. We have introduced the order parameter $\Delta_{\boldsymbol{k}}(\boldsymbol{r},t) = \sum_{\boldsymbol{k}'} V_{\boldsymbol{k}-\boldsymbol{k}'} p_{\boldsymbol{k}'}(\boldsymbol{r},t) - g\lambda_{cav}(\boldsymbol{r},t)$ describing the condensed phase, where $\lambda_{cav}(\boldsymbol{r},t) = \langle a(\boldsymbol{r},t)\rangle$ is the coherent cavity-photon amplitude [where $a(\boldsymbol{r},t)$ is the annihilation operator of a cavity photon], $V_{\boldsymbol{k}} = e^2/(2\epsilon|\boldsymbol{k}|)$ is the two-dimensional Coulomb interaction (ϵ is the dielectric constant), and g is a dipole coupling between carriers (electrons and holes) and photons. The coupling of the system to the bath causes the dephasing (decay) of $p_{\boldsymbol{k}}(\boldsymbol{r},t)$ ($n_{\boldsymbol{k},\sigma}(\boldsymbol{r},t)$) with the rate 2γ ($2\gamma_\sigma$), where $\gamma = (\gamma_e+\gamma_h)/2$. $L_{\boldsymbol{k},\boldsymbol{k}'}(\boldsymbol{r},t)$ and $I_{\boldsymbol{k},\sigma}(\boldsymbol{r},t)$ in Eqs. (1) and (2), determined microscopically from the self-energy $\hat{\Sigma}$ and the Green's function $\hat{G}$ in the Nambu-Keldysh formalism (see SM [53] for their explicit form), describe many-body interaction effects such as exciton formation, collision, phase filling etc., as well as the electron-hole pumping and its thermalization.

The electron-hole dynamics is coupled to the dynamics of the coherent cavity-photon amplitude, given by the Heisenberg equation [53],

$$i\hbar\partial_t\lambda_{cav}(\boldsymbol{r},t) = \langle[a(\boldsymbol{r},t),H]\rangle = \left(\hbar\omega_{cav} - \frac{\hbar^2\nabla^2}{2m_{cav}} - i\kappa\right)\times\lambda_{cav}(\boldsymbol{r},t) + g\sum_{\boldsymbol{k}} p_{\boldsymbol{k}}(\boldsymbol{r},t), \tag{3}$$

where $\hbar\omega_{cav}$ is the cavity-photon energy, and m_{cav} is a cavity-photon mass. In analogy to $\lambda_{cav}(\boldsymbol{r},t)$, we define for later use a complex electron-hole pair amplitude $\lambda_{eh}(\boldsymbol{r},t)$ by $p_{\boldsymbol{k}}(\boldsymbol{r},t) = \lambda_{eh}(\boldsymbol{r},t)\phi_{\boldsymbol{k}}(\boldsymbol{r},t)$, $\sum_{\boldsymbol{k}}|\phi_{\boldsymbol{k}}(\boldsymbol{r},t)|^2 = 1$, $\mathrm{Arg}[\sum_{\boldsymbol{k}}\phi_{\boldsymbol{k}}(\boldsymbol{r},t)] = 0$ [56].

Our main assumption in what follows is that the system supports spatially uniform, steady-state solutions given by the ansatz [30–34,48,57,58] $\lambda_{\mathrm{cav(eh)}}(t)=\lambda^0_{\mathrm{cav(eh)}}e^{-iEt/\hbar}$, where E is the (real) condensate emission energy. Although, in real systems, there is always a chance that such a uniform steady state destabilizes, e.g., due to the dynamical instability that leads to pattern formation [59–61] or the occurrence of many-body localization [62], we ignore such possibilities in this Letter. In this formulation, $\lambda^0_{\mathrm{cav(eh)}}$ corresponds to the photonic (excitonic) component of the macroscopic many-body wave function.

With this ansatz, Eqs. (1) and (3) satisfy a non-Hermitian eigenvalue equation,

$$\hat{A}\begin{pmatrix}\lambda^0_{\mathrm{cav}}\\ \lambda^0_{\mathrm{eh}}\end{pmatrix}=\begin{pmatrix}h_{\mathrm{cav}} & g_0\\ \tilde{g}_0^* & h_{\mathrm{eh}}\end{pmatrix}\begin{pmatrix}\lambda^0_{\mathrm{cav}}\\ \lambda^0_{\mathrm{eh}}\end{pmatrix}=E\begin{pmatrix}\lambda^0_{\mathrm{cav}}\\ \lambda^0_{\mathrm{eh}}\end{pmatrix}, \quad (4)$$

where $h_{\mathrm{cav}}=\hbar\omega_{\mathrm{cav}}-i\kappa$, $g_0=g\sum_{\boldsymbol{k}}\phi_{\boldsymbol{k}}$, $\tilde{g}_0^*=g\sum_{\boldsymbol{k},\boldsymbol{k}'}\phi^*_{\boldsymbol{k}}L_{\boldsymbol{k},\boldsymbol{k}'}$, and $h_{\mathrm{eh}}=\sum_{\boldsymbol{k}}[(\varepsilon_{\boldsymbol{k},\mathrm{e}}+\varepsilon_{\boldsymbol{k},\mathrm{h}}-2i\gamma)|\phi_{\boldsymbol{k}}|^2-\sum_{\boldsymbol{p},\boldsymbol{k}'}V_{\boldsymbol{k}-\boldsymbol{p}}\phi^*_{\boldsymbol{k}}\phi_{\boldsymbol{p}}L_{\boldsymbol{k},\boldsymbol{k}'}]$. We emphasize that Eq. (4) is a steady state condition that determines the macroscopic variables $\lambda^0_{\mathrm{cav(eh)}}$ and is analogous to a gap equation, not to be confused [63] with the equations for determining the polariton spectra in the normal state [6]. For instance, the trivial solution $\lambda^0_{\mathrm{cav}}=\lambda^0_{\mathrm{eh}}=0$ describes the normal state.

Equations (1)–(3) must be solved self-consistently for a given set of microscopic parameters to determine the quantities that enter Eq. (4) [69]. However, we can draw a number of strong conclusions by analyzing the structure of the latter alone. The matrix $\hat{A}$ can be diagonalized with eigenvectors $\boldsymbol{u}_-=[(-\varphi+\Omega/2),-\tilde{g}_0^*]^{\mathsf{T}}$, $\boldsymbol{u}_+=[g_0,(-\varphi+\Omega/2)]^{\mathsf{T}}$, and corresponding eigenvalues $E_\pm=[h_{\mathrm{cav}}+h_{\mathrm{eh}}\pm\Omega]/2$. Here, $\Omega=\sqrt{\varphi^2+4\tilde{g}_0^*g_0}$, $\varphi=h_{\mathrm{cav}}-h_{\mathrm{eh}}$, and we take $\mathrm{Re}\Omega\geq 0$ (i.e., $\mathrm{Re}E_+\geq\mathrm{Re}E_-$) without loss of generality. In the diagonal basis, Eq. (4) reads $(E_--E)\lambda^0_-=(E_+-E)\lambda^0_+=0$, where $(\lambda^0_-,\lambda^0_+)^{\mathsf{T}}=\hat{U}(\lambda^0_{\mathrm{cav}},\lambda^0_{\mathrm{eh}})^{\mathsf{T}}$ with $\hat{U}^{-1}=(\boldsymbol{u}_-,\boldsymbol{u}_+)$. From this relation, we see that λ^0_- and λ^0_+ cannot be nonzero simultaneously as long as $E_-\neq E_+$, allowing us to classify the nontrivial solutions into two types: $(\lambda^0_-\neq 0,\lambda^0_+=0,E=E_-)$ and $(\lambda^0_+\neq 0,\lambda^0_-=0,E=E_+)$, which we label "−" and "+", respectively. This property is essentially different from similar time-dependent coupled-damped oscillator equations, $i\partial_t(\psi_1,\psi_2)^{\mathsf{T}}=\hat{H}_{\mathrm{cdo}}(\psi_1,\psi_2)^{\mathsf{T}}$ (where ψ_1 and ψ_2 are complex numbers and $\hat{H}_{\mathrm{cdo}}$ is a non-Hermitian 2×2 matrix), which are often discussed in the field of non-Hermitian quantum mechanics [36–43], where the transient dynamics generally allows for a superposition of eigenmodes.

Now we show our main result of this Letter: A first-order-like phase transition between the two solutions can occur and the EP $\Omega=0$, where $\boldsymbol{u}_\pm$ coalesce such that $\hat{A}$ only has a single eigenvector, marks the end point of the phase boundary. The proof is presented in the SM [53] and we sketch the argument here. Introducing the complex splitting between E_- and E_+,

$$\Lambda\equiv\Omega^2=\varphi^2+4\tilde{g}_0^*g_0, \quad (5)$$

we divide the complex Λ plane into the regions I–IV, according to the strong-coupling condition [70] $\tilde{\delta}^2+4\mathrm{Re}[\tilde{g}_0^*g_0]\geq 4\kappa^2$ (where $\tilde{\delta}=\mathrm{Re}\varphi$) and the sign of $\mathrm{Im}\Lambda$, as shown in Fig. 3(a) [71]. Because of the restriction of real E, only one solution type can exist in the weak-coupling regime (regions II and III), which switches label with no physical discontinuity between regions II and III. On the other hand, both (distinct) solution types may coexist in the strong-coupling regions I and IV. Thus, starting from the "−" solution in region III, while no discontinuity would be seen when entering region II directly, changing parameters in a route that encircles the EP (III → IV → I → II) requires a phase transition in order to end up in the required "+" solution in region II, proving the result [72].

To make contact between the above general arguments and real physical systems, we explicitly solve for the polariton BEC and VCSEL. In the dilute equilibrium limit $(\kappa=0,\gamma\to 0^+,n_{k,\sigma}\ll 1)$ where the polariton BEC is realized, Eq. (4) reduces to [53]

$$\hat{A}_{\mathrm{BEC}}=\begin{pmatrix}\hbar\omega_{\mathrm{cav}} & g_{\mathrm{R}}\\ g_{\mathrm{R}}^* & \hbar\omega_{\mathrm{X}}\end{pmatrix}, \quad (6)$$

in the Hartree-Fock-Bogoliubov approximation (HFBA) [32–34,48], which is justified in this limit [73]. Here, $\hbar\omega_{\mathrm{X}}=E_{\mathrm{g}}-E_{\mathrm{X}}^{\mathrm{bind}}$ is the exciton energy ($E_{\mathrm{X}}^{\mathrm{bind}}$ is the exciton binding energy) and $g_{\mathrm{R}}=g\phi_{\mathrm{X}}(\boldsymbol{r}=0)$ is the Rabi splitting, where $\phi_{\mathrm{X}}(\boldsymbol{r})$ is an exciton wave function obeying the Schrödinger equation $\int d\boldsymbol{r}'[-\delta(\boldsymbol{r}-\boldsymbol{r}')\hbar^2\nabla'^2/m_{\mathrm{eh}}-V(\boldsymbol{r}-\boldsymbol{r}')]\phi_{\mathrm{X}}(\boldsymbol{r}')=-E_{\mathrm{X}}^{\mathrm{bind}}\phi_{\mathrm{X}}(\boldsymbol{r})$ [73]. The eigenvalues, given by

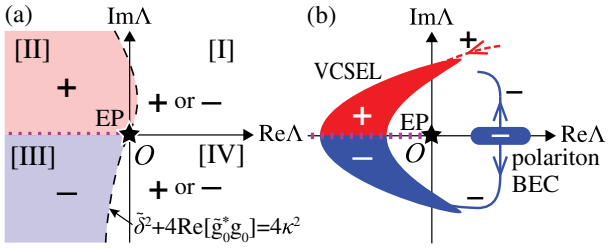

FIG. 3. (a) Definition of regions I–IV. In region II (III) in the weak-coupling regime, only the "+(−)" solution is allowed. On the dotted line, the solution type switches without being accompanied by discontinuity. (b) Schematic description of how a polariton BEC evolves to a VCSEL, in terms of Λ. The system exhibits a phase transition (crossover) from a polariton BEC to a VCSEL when Λ changes counterclockwise (clockwise) around EP.

$E_{\pm}^{\mathrm{BEC}} = [\hbar\omega_{\mathrm{cav}} + \hbar\omega_{\mathrm{X}} \pm \sqrt{\delta^2 + 4|g_R|^2}]/2$, are just the lower and upper polariton energies [6] (where $\delta = \hbar\omega_{\mathrm{cav}} - \hbar\omega_{\mathrm{X}}$ is the conventional detuning parameter). Comparison of the free energies of the two solutions tells us that the "−" solution always emerges.

When the photon decay rate κ is turned on, a phase transition can occur. In the so-called polariton laser regime, where the gas is dilute enough to maintain the polariton picture, the equation of motion is governed by the driven-dissipative Gross-Pitaevskii (ddGP) equation [74] generalized to the two-component case, given by [53]

$$\hat{A}_{\mathrm{GP}} = \begin{pmatrix} \hbar\omega_{\mathrm{cav}} - i\kappa & g_R \\ g_R^* & \hbar\omega_{\mathrm{X}} + U_{\mathrm{X}}|\lambda_{\mathrm{eh}}^0|^2 + iR_{\mathrm{X}} \end{pmatrix}, \quad (7)$$

where U_{X} is an exciton-exciton interaction strength and $R_{\mathrm{X}} > 0$ describes the net gain of exciton coherence that feeds the condensate [75], arising microscopically from processes such as stimulated scattering. This gives $E_{\pm}^{\mathrm{GP}} = [\hbar\omega_{\mathrm{cav}} + \hbar\omega_{\mathrm{X}} + U_{\mathrm{X}}|\lambda_{\mathrm{eh}}^0|^2 - i(\kappa - R_{\mathrm{X}}) \pm \Omega_{\mathrm{GP}}]/2$ with $\Omega_{\mathrm{GP}} = \sqrt{\tilde{\delta}^2 + 4|g_R|^2 - (\kappa + R_{\mathrm{X}})^2 - 2i\tilde{\delta}(\kappa + R_{\mathrm{X}})}$, where $\tilde{\delta} = \hbar\omega_{\mathrm{cav}} - (\hbar\omega_{\mathrm{X}} + U_{\mathrm{X}}|\lambda_{\mathrm{eh}}^0|^2)$ is an effective detuning that takes into account the Hartree shift of the exciton component. One finds an EP ($\Omega_{\mathrm{GP}} = 0$) at $\tilde{\delta} = 0$ and $g_R = R_{\mathrm{X}} = \kappa$, giving rise to a phase transition in its vicinity.

We demonstrate this by explicitly solving Eq. (4) when $\hat{A} = \hat{A}_{\mathrm{GP}}$. Figure 4 shows the calculated emission energy E as a function of the decay rate κ and the coherent photon number $n_{\mathrm{ph}}^0 = |\lambda_{\mathrm{cav}}^0|^2$ (which roughly corresponds to the pump power), in the blue detuning case $\delta/g_R = 0.1$. At $\kappa < g_R$, we find that the "−" solution disappears at a critical value of the pump power, resulting in a phase transition signaled by the discontinuity in E. In constructing the phase diagram, we have assumed that we always realize the lowest-energy solution. Relaxing this assumption would shift the position of the phase boundary in detail but not its end point. As expected, the phase boundary ends at the EP (where $\kappa = g_R$). When $\kappa > g_R$, the "−" solution crosses over to the "+" solution. The fact that a phase transition arises within the ddGP (where the polariton picture still holds) suggests that the second threshold observed in experiments does not necessarily imply a strong-to-weak-coupling transition to a photon laser. More discussion on this aspect can be found in the SM [53].

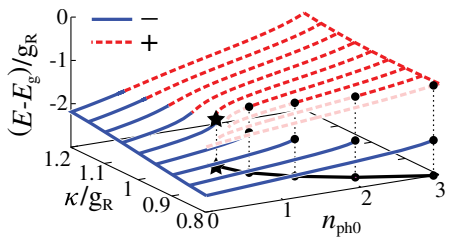

FIG. 4. Calculated emission energy E in the case $\hat{A} = \hat{A}_{\mathrm{GP}}$ as a function of the photon decay rate κ/g_{R} and the (coherent) photon number $n_{\mathrm{ph}}^0 = |\lambda_{\mathrm{cav}}^0|^2$. The solid line projected onto the n_{ph}^0-κ/g_{R} plane is a phase boundary. The star represents the EP. We set $\delta/g_{\mathrm{R}} = 0.1, \hbar\omega_{\mathrm{X}}/g_{\mathrm{R}} = -2, U_{\mathrm{X}}/g_{\mathrm{R}} = 0.1$.

At high pump power where the system operates as a VCSEL, it has been shown within the HFBA [32–34] that Eqs. (1)–(3) reduce to the semiconductor Maxwell-Bloch equations [15], with $L_{\boldsymbol{k},\boldsymbol{k}'} = \delta_{\boldsymbol{k},\boldsymbol{k}'}N_{\boldsymbol{k}} = \delta_{\boldsymbol{k},\boldsymbol{k}'}(1 - n_{\boldsymbol{k},\mathrm{e}} - n_{\boldsymbol{k},\mathrm{h}})$ and

$$\hat{A}_{\mathrm{VL}} = \begin{pmatrix} \hbar\omega_{\mathrm{cav}} - i\kappa & g_0 \\ \tilde{g}_0^{\mathrm{VL}_*} & \hbar\omega_{\mathrm{eh}}^{\mathrm{VL}} - 2i\gamma \end{pmatrix}, \quad (8)$$

where $\hbar\omega_{\mathrm{eh}}^{\mathrm{VL}} = \sum_{\boldsymbol{k}}[(\varepsilon_{\boldsymbol{k},\mathrm{e}} + \varepsilon_{\boldsymbol{k},\mathrm{h}})|\phi_{\boldsymbol{k}}|^2 - \sum_{\boldsymbol{p}} V_{\boldsymbol{k}-\boldsymbol{p}}\phi_{\boldsymbol{k}}^*\phi_{\boldsymbol{p}}N_{\boldsymbol{k}}]$ and $\tilde{g}_0^{\mathrm{VL}_*} = g\sum_{\boldsymbol{k}}\phi_{\boldsymbol{k}}^*N_{\boldsymbol{k}}$. A crucial difference compared to the polariton laser case, Eq. (7), is the condensate feeding mechanism. The electron-hole gain $R_{\mathrm{X}}(> 0)$ present in the polariton laser is absent in the VCSEL, since the thermalization process does not work efficiently. Instead, the condensate is fed by stimulated emission arising from the population inversion $N_{\boldsymbol{k}} < 0$. As a result, it is straightforward to show [53] that $\mathrm{Re}\Lambda_{\mathrm{VL}} < 0$ holds when $\mathrm{Im}\Lambda_{\mathrm{VL}} = 0$ in the weak-coupling regime [76], allowing both the solution types to appear and smoothly switch labels with one another.

Figure 3(b) summarizes the above discussion in terms of the complex splitting Λ. Here, the polariton BEC regime lies on the real axis $\Lambda_{\mathrm{BEC}} = \delta^2 + |g_R|^2 > 0$. Thus, starting from the polariton BEC with "−" solution, by changing parameters such that Λ evolves clockwise or counterclockwise around the EP, the system exhibits a crossover or phase transition, respectively, into a VCSEL.

We connect our discussion in Λ space to the physical phase diagram in Fig. 1. Starting from the polariton BEC ($\kappa = 0$), as the decay rate κ is turned on such that the system turns into a polariton laser [Eq. (7)], one sees from the expression of $\Lambda_{\mathrm{GP}} = \Omega_{\mathrm{GP}}^2$ that $\mathrm{Im}\Lambda$ increases (decreases) from zero in the case of an effective red (blue) detuning $\tilde{\delta} < 0$ (> 0), where Λ evolves counterclockwise (clockwise). Since the increasing pump power P usually shifts the effective detuning to red (note that $\tilde{\delta} = \delta - U_{\mathrm{X}}|\lambda_{\mathrm{eh}}^0|^2$), we predict that there always exists a phase boundary between the polariton BEC and VCSEL in red detuning, $\delta < 0$ [Fig. 1(c)]. On the other hand, in blue detuning, $\delta > 0$, $\tilde{\delta}$ may switch its sign to negative when P increases. Whether this sign change occurs at a positive or negative $\mathrm{Re}\Lambda$ determines whether the evolution of Λ may reverse to counterclockwise. Thus, we conjecture that, in the blue detuning case, there exists a phase boundary with an end point, as shown in Fig. 1(a). On resonance, $\delta = 0$, since we know from Eq. (7) that the EP is at $\kappa = g_{\mathrm{R}}$ in the dilute limit

$|\lambda^0_{\rm eh}| \to 0$ ($\tilde{\delta} = \delta = 0$), the EP lies on the boundary between the normal and the condensed phase [Fig. 1(b)].

Physically, when the effective detuning becomes more red, the lower branch becomes more photonic [6], hindering condensation to the lower branch as photonic losses increase and gain from the excitonic component becomes small. Meanwhile, the upper branch becomes more excitonic, which makes the system favor the latter and eventually driving the phase transition. In contrast, as long as the system stays in effective blue detuning, it remains in the "−" solution, exhibiting a crossover.

We close our Letter by commenting on the connection to experiments. Most reported experiments exhibiting the two-threshold behavior are done on resonance or in red detuning with a small decay rate $\kappa < g_{\rm R}$ [18–28], while a single-threshold behavior to a photon laser has been observed at a large blue detuning [17]. These results are consistent with our proposal (more detailed discussion is provided in the SM [53]) which makes us hopeful that an experimental encirclement of the EP is within reach.

We thank S. Diehl, D. Myers, S. Mukherjee, M. Yamaguchi, K. Kamide, T. Ogawa, and K. Asano for discussions. This work was supported by KiPAS project in Keio University. R. H. was supported by a Grand-in-Aid for JSPS fellows (Grant No. 17J01238). Y. O. was supported by Grant-in-Aid for Scientific Research from MEXT and JSPS in Japan (No. JP18K11345, No. JP18H05406, No. JP16K05503). Work at Argonne National Laboratory is supported by the U.S. Department of Energy, Office of Science, BES-MSE under Contract No. DE-AC02-06CH11357.

*hanai@acty.phys.sci.osaka-u.ac.jp

[1] N. P. Proukakis, D. W. Snoke, and P. B. Littlewood, *Universal Themes of Bose-Einstein Condensation* (Cambridge Univesity Press, Cambridge, England, 2017).
[2] M. H. Anderson, J. R. Ensher, M. R. Mattews, C. E. Wieman, and E. A. Cornell, Science **269**, 198 (1995).
[3] K. B. Davis, M.-O. Mewes, M. R. Andrews, N. J. van Druten, D. S. Durfee, D. M. Kurn, and W. Ketterle, Phys. Rev. Lett. **75**, 3969 (1995).
[4] K. Huang, *Statistical Mechanics*, 2nd ed. (Wiley, New York, 1987).
[5] J. Kasprzak, M. Richard, S. Kundermann, A. Baas, P. Jeambrun, J. Keeling, F. M. Marchetti, M. H. Szymańska, R. André, J. L. Staehli, V. Savona, P. B. Littlewood, B. Deveaud, and L. S. Dang, Nature (London) **443**, 409 (2006).
[6] H. Deng, H. Haug, and Y. Yamamoto, Rev. Mod. Phys. **82**, 1489 (2010).
[7] I. Carusotto and C. Ciuti, Rev. Mod. Phys. **85**, 299 (2013).
[8] T. Byrnes, N. Y. Kim, and Y. Yamamoto, Nat. Phys. **10**, 803 (2014).
[9] Ch. Rüegg, N. Cavadini, A. Furrer, H.-U. Güdel, K. Krämer, H. Mutka, A. Wildes, K. Habicht, and P. Vorderwisch, Nature (London) **423**, 62 (2003).
[10] S. O. Demokritov, V. E. Devidov, O. Dzyapko, G. A. Melkov, A. A. Serga, B. Hillebrands, and A. N. Slavin, Nature (London) **443**, 430 (2006).
[11] A. V. Chumak, G. A. Melkov, V. E. Demidov, O. Dzyapko, V. L. Safonov, and S. O. Demokritov, Phys. Rev. Lett. **102**, 187205 (2009).
[12] J. Klaers, J. Schmitt, F. Vewinger, and M. Weitz, Nature (London) **468**, 545 (2010).
[13] T. K. Hakala, A. J. Moilanen, A. I. Väkeväinen, R. Guo, J-P. Martikainen, K. S. Daskalakis, H. T. Rekola, A. Julku, and P. Törmä, Nat. Phys. **14**, 739 (2018).
[14] M. O. Scully and M. S. Zubairy, *Quantum Optics*, (Cambridge University Press, Cambridge, England, 1997).
[15] H. Haug and S. W. Koch, *Quantum Theory of the Optical and Electronic Properties of Semicoductors* (World Scientific, Singapore, 2009).
[16] A. Imamoglu, R. J. Ram, S. Pau, and Y. Yamamoto, Phys. Rev. A **53**, 4250 (1996).
[17] H. Deng, G. Weihs, D. Snoke, J. Bloch, and Y. Yamamoto, Proc. Natl. Acad. Sci. U.S.A. **100**, 15318 (2003).
[18] D. Bajoni, P. Senellart, E. Wertz, I. Sagnes, A. Miard, A. Lemaître, and J. Bloch, Phys. Rev. Lett. **100**, 047401 (2008).
[19] R. Balili, B. Nelsen, D. W. Snoke, L. Pfeiffer, and K. West, Phys. Rev. B **79**, 075319 (2009).
[20] B. Nelsen, R. Balili, D. W. Snoke, L. Pfeiffer, and K. West, J. Appl. Phys. **105**, 122414 (2009).
[21] J. S. Tempel, F. Veit, M. Aßmann, L. E. Kreilkamp, A. Rahimi-Iman, A. Löffler, S. Höfling, S. Reitzenstein, L. Worschech, A. Forchel, and M. Bayer, Phys. Rev. B **85**, 075318 (2012).
[22] J. S. Tempel, F. Veit, M. Aßmann, L. E. Kreilkamp, S. Höfling, M. Kamp, A. Forchel, and M. Bayer, New J. Phys. **14**, 083014 (2012).
[23] P. Tsotsis, P. S. Eldridge, T. Gao, S. I. Tsintzos, Z. Hatzopoulos, and P. G. Savvidis, New J. Phys. **14**, 023060 (2012).
[24] T. Horikiri, Y. Matsuo, Y. Shikano, A. Löffler, S. Höfling, A. Forchel, and Y. Yamamoto, J. Phys. Soc. Jpn. **82**, 084709 (2013).
[25] C. Schneider, A. Rahimi-Iman, N. Y. Kim, J. Fischer, I. G. Savenko, M. Amthor, M. Lermer, A. Wolf, L. Worschech, V. D. Kulakovskii, I. A. Shelykh, M. Kamp, S. Reitzenstein, A. Forchel, Y. Yamamoto, and S. Höfling, Nature (London) **497**, 348 (2013).
[26] J. Fischer, S. Brodbeck, A. V. Chernenko, I. Lederer, A. Rahimi-Iman, M. Amthor, V. D. Kulakovskii, L. Worschech, M. Kamp, M. Durnev, C. Schneider, A. V. Kavokin, and S. Höfling, Phys. Rev. Lett. **112**, 093902 (2014).
[27] S. Brodbeck, H. Suchomel, M. Amthor, T. Steinl, M. Kamp, C. Schneider, and S. Höfling, Phys. Rev. Lett. **117**, 127401 (2016).
[28] S. Kim, B. Zhang, Z. Wang, J. Fischer, S. Brodbeck, M. Kamp, C. Schneider, S. Höfling, and H. Deng, Phys. Rev. X **6**, 011026 (2016).
[29] C. P. Dietrich, A. Steude, L. Tropf, M. Schubert, N. M. Kronenberg, K. Ostermann, S. Höfling, and M. C. Gather, Sci. Adv. **2**, e1600666 (2016).
[30] M. H. Szymańska, J. Keeling, and P. B. Littlewood, Phys. Rev. Lett. **96**, 230602 (2006).

[31] M. H. Szymańska, J. Keeling, and P. B. Littlewood, Phys. Rev. B **75**, 195331 (2007).

[32] M. Yamaguchi, K. Kamide, T. Ogawa, and Y. Yamamoto, New J. Phys. **14**, 065001 (2012).

[33] M. Yamaguchi, K. Kamide, R. Nii, T. Ogawa, and Y. Yamamoto, Phys. Rev. Lett. **111**, 026404 (2013).

[34] M. Yamaguchi, R. Nii, K. Kamide, T. Ogawa, and Y. Yamamoto, Phys. Rev. B **91**, 115129 (2015).

[35] T. Kato, *Perturbation Theory of Linear Operators* (Springer, Berlin, 1966).

[36] C. M. Bender and S. Boettcher, Phys. Rev. Lett. **80**, 5243 (1998).

[37] W. D. Heiss, Eur. Phys. J. D **7**, 1 (1999).

[38] C. Dembowski, B. Dietz, H.-D. Gräf, H. L. Harney, A. Heine, W. D. Heiss, and A. Richter, Phys. Rev. E **69**, 056216 (2004).

[39] W. D. Heiss, J. Phys. A **37**, 2455 (2004).

[40] W. D. Heiss, J. Phys. A **45**, 444016 (2012).

[41] C. Dembowski, H.-D. Gräf, H. L. Harney, A. Heine, W. D. Heiss, H. Rehfeld, and A. Richter, Phys. Rev. Lett. **86**, 787 (2001).

[42] S.-B. Lee, J. Yang, S. Moon, S.-Y. Lee, J.-B. Shim, S. W. Kim, J.-H. Lee, and K. An, Phys. Rev. Lett. **103**, 134101 (2009).

[43] T. Gao, E. Estrecho, K. Y. Bliokh, T. C. H. Liew, M. D. Fraser, S. Brodbeck, M. Kamp, C. Schneider, S. Höfling, Y. Yamamoto, F. Nori, Y. S. Kivshar, A. G. Truscott, R. G. Dall, and E. A. Ostrovskaya, Nature (London) **526**, 554 (2015).

[44] E. Graefe, J. Phys. A **45**, 444015 (2012).

[45] H. Cartarius and G. Wunner, Phys. Rev. A **86**, 013612 (2012).

[46] D. Dast, D. Haag, H. Cartarius, G. Wunner, R. Eichler, and J. Main, Fortschr. Phys. **61**, 124 (2013).

[47] J. Léonard, A. Morales, P. Zupancic, T. Esslinger, and T. Donner, Nature (London) **543**, 87 (2017).

[48] R. Hanai, P. B. Littlewood, and Y. Ohashi, Phys. Rev. B **97**, 245302 (2018).

[49] References [32–34] have shown within the Hartree-Fock-Bogoliubov approximation that taking the equilibrium limit of Eqs. (1)–(3) yields the gap equation of the Bardeen-Cooper-Schrieffer theory that describes an electron-hole-photon condensate in equilibrium, and at a high-density regime, these equations collapse to the semiconductor Maxwell Bloch equations that describes a VCSEL.

[50] M. Aßmann, J. Tempel, F. Veit, M. Bayer, A. Rahimi-Iman, A. Löffler, S. Höfling, S. Reitzenstein, L. Worschech, and A. Forchel, Proc. Natl. Acad. Sci. U.S.A. **108**, 1804 (2011).

[51] M. Nakayama, K. Murakami, and D. Kim, J. Phys. Soc. Jpn. **85**, 054702 (2016).

[52] M. Nakayama and M. Ueda, Phys. Rev. B **95**, 125315 (2017).

[53] See Supplemental Material at http://link.aps.org/supplemental/10.1103/PhysRevLett.122.185301 for details. These include (1) the explicit expression of the Hamiltonian H, (2) microscopic derivation of Eqs. (1)–(3), (3) proof on the existence of a phase boundary with an end point, (4) analysis in various regimes, and (5) implications of our results for experiments.

[54] J. Rammer, *Quantum Field Theory of Non-Equilibrium States* (Cambridge University Press, Cambridge, England, 2007).

[55] L. P. Kadanoff and G. Baym, *Quantum Statistical Mechanics* (Benjamin, New York, 1962).

[56] C. Comte and P. Nozières, J. Phys. (Les Ulis, Fr.) **43**, 1069 (1982).

[57] R. Hanai, P. B. Littlewood, and Y. Ohashi, Phys. Rev. B **96**, 125206 (2017).

[58] R. Hanai, P. B. Littlewood, and Y. Ohashi, J. Low Temp. Phys. **183**, 127 (2016).

[59] K. S. Daskalakis, S. A. Maier, and S. Kéna-Cohen, Phys. Rev. Lett. **115**, 035301 (2015).

[60] N. Bobrovska, M. Matuszewski, K. S. Daskalakis, S. A. Maier, and S. Kéna-Cohen, ACS Photonics **5**, 111 (2018).

[61] F. Baboux, D. D. Bernardis, V. Goblot, V. N. Gladilin, C. Gomez, E. Galopin, L. L. Gratiet, A. Lemaître, I. Sagnes, I. Carusotto, M. Wouters, A. Amo, and J. Bloch, Optica **5**, 1163 (2018).

[62] T. J. Sturges, M. D. Anderson, A. Buraczewski, M. Navadeh-Toupchi, A. F. Adiyatullin, F. Jabeen, D. Y. Oberli, M. T. Portella-Oberli, and M. Stobińska, arXiv:1903.09550.

[63] The usual polariton spectrum in the normal state is recovered by considering the dynamics of the thermally excited fluctuations $\delta\lambda_{\mathrm{cav/eh}}(\boldsymbol{r},t)=[\lambda_{\mathrm{cav/eh}}(\boldsymbol{r},t)-\lambda^0_{\mathrm{cav/eh}}]e^{-iEt/\hbar}$ around the steady state solution $\lambda^0_{\mathrm{cav}}=\lambda^0_{\mathrm{eh}}=0$. These noncondensed polariton formations are included in the many-body collision term I through the self-energy $\hat{\Sigma}$, which is well known to be captured by including the ladder diagrams [64–68]. Since our general framework can in principle take into account *all* the diagrams including the above, these noncondensed polariton formations are well captured in our theory.

[64] R. Zimmermann, K. Kilimann, W. D. Kraeft, D. Kremp, and G. Röpke, Phys. Status Solidi (b) **90**, 175 (1978).

[65] N. H. Kwong, G. Rupper, and R. Binder, Phys. Rev. B **79**, 155205 (2009).

[66] K. Asano and T. Yoshioka, J. Phys. Soc. Jpn. **83**, 084702 (2014).

[67] J. Keeling, P. R. Eastham, M. H. Szymańska, and P. B. Littlewood, Phys. Rev. B **72**, 115320 (2005).

[68] Y. Ohashi and A. Griffin, Phys. Rev. A **67**, 063612 (2003).

[69] Precisely speaking, our assumption is that the Dyson's equation (where its explicit form is given in the SM [53]) is solved to obtain all the terms in Eqs. (1)–(3).

[70] V. Savona, L. C. Andreani, P. Schwendimann, and A. Quattropani, Solid State Commun. **93**, 733 (1995).

[71] It is shown in the SM [53] that the strong-coupling regime $\tilde{\delta}^2+4\mathrm{Re}[\tilde{g}_0^*g_0]\geq 4\kappa^2$ is realized at $\mathrm{Re}\Lambda\geq 0$, at least in the vicinity of $\mathrm{Im}\Lambda=0$.

[72] We have implicitly assumed that $\hat{A}$ is a smooth function of the input parameters and has maximum of one solution per solution type.

[73] In deriving Eq. (6), we have assumed $g_{\mathrm{R}}\ll E_{\mathrm{X}}^{\mathrm{bind}}$, for simplicity.

[74] M. Wouters and I. Carusotto, Phys. Rev. Lett. **99**, 140402 (2007).

[75] The nonlinearity and the gain is present only in the diagonal exciton component under the condition $g_{\mathrm{R}}\ll E_{\mathrm{X}}^{\mathrm{bind}}$ [53].

[76] Here, we have assumed that the VCSEL is in an extremely strong pumping regime where a large population inversion $N_{\boldsymbol{k}}\simeq -1$ exists at a predominant momentum window, which makes $\hbar\omega_{\mathrm{eh}}^{\mathrm{VL}}\simeq\sum_{\boldsymbol{k}}[(\varepsilon_{\boldsymbol{k},\mathrm{e}}+\varepsilon_{\boldsymbol{k},\mathrm{h}})|\phi_{\boldsymbol{k}}|^2+\sum_{\boldsymbol{p}}V_{\boldsymbol{k}-\boldsymbol{p}}\phi^*_{\boldsymbol{k}}\phi_{\boldsymbol{p}}$ a real number and $\tilde{g}_0^{\mathrm{VL}_*}\simeq -g_0^*$.